Journal of Sustainable Cement-Based Materials

ISSN: 2165-0373 (Print) 2165-0381 (Online) Journal homepage: https://www.tandfonline.com/loi/tscm20

Effect of interparticle action on shear thickening behavior of cementitious composites: modeling and experimental validation

Xuhao Wang, Alan Lu & Kejin Wang

To cite this article: Xuhao Wang, Alan Lu & Kejin Wang (2020) Effect of interparticle action on shear thickening behavior of cementitious composites: modeling and experimental validation, Journal of Sustainable Cement-Based Materials, 9:2, 78-93, DOI: 10.1080/21650373.2019.1692257

To link to this article: https://doi.org/10.1080/21650373.2019.1692257

Journal of Sustainable Cement-Based Materials, 2020
Vol. 9, No. 2, 78–93, http://dx.doi.org/10.1080/21650373.2019.1692257

Effect of interparticle action on shear thickening behavior of cementitious composites: modeling and experimental validation

Xuhao Wang[a,b,c], Alan Lu[d]*, and Kejin Wang[e]

[a]*Research and Development Center of Transport Industry of Technologies, Materials and Equipment of Highway Construction and Maintenance, Gansu Road & Bridge Construction, Gansu, China;* [b]*School of Highway, Chang an University, Xi an, China;* [c]*Key Laboratory of Special Area Highway Engineering, Ministry of Education, Xi an, China;* [d]*US Department of Labor, Washington DC, 20210, US;* [e]*Department of Civil, Construction and Environmental Engineering, Iowa State University, Ames, IA, USA*

Shear thickening is a behavior of a material that displays an increase in viscosity with increasing shear rate. Research has indicated that in self-consolidating concrete (SCC), shear thickening is primarily caused by the formation of "particle clusters" due to collisions of particles in the low yield stress of the fluid material matrix of SCC at a high flow rate. Based on this theory, a previously developed particle–fluid model was modified and applied to predict the relationship between the shear stress and shear strain rate of cementitious composites that exhibit shear thickening behavior. The rheology test results indicated no apparent shear thickening behavior was observed for SCC paste mixtures while distinct shear thickening behavior was observed when the introduced fine aggregate volume fraction increased up to 40%. The modified model showed a power function between the shear stress and shear rate that could well capture the shear thickening behavior of mortar mixtures with various aggregate volume fractions and that agreed well with the results of the experimental study. The modified model also demonstrated that aggregate particles could generate local transient particle clusters during interactions due to the particles' varying velocities, yielding shear thickening.

Keywords: Cementitious composite, shear thickening, interparticle force, shear stress

1. Introduction

Self-consolidating concrete (SCC) can flow and fill formwork under its own weight and can reach full compaction without additional consolidation, such as vibration [1]. Applications of SCC in today's construction industry depend upon its flow properties. Such properties of SCC include flowability, filling ability, and pumpability [2,3].

Shear thickening is a phenomenon in which the viscosity of the composite increases with an increased shear rate [4]. When shear thickening occurs, it becomes more difficult to mix and pump concrete because of the increased energy required for concrete flow. It has been reported that shear thickening behavior has been observed in SCC applications [5,6]. In many cases, this undesirable shear thickening behavior limits the application of SCC where pumping is essential.

From the rheology point of view, the majority of investigations of shear

*Corresponding author. Email: 86015990@qq.com Department of Labor, Washington DC, 20210, US

This article has been republished with minor changes. These changes do not impact the academic content of the article.

thickening have been conducted on colloidal suspensions. The detailed mechanisms of shear thickening are still controversial [7–14]. Two different mechanisms have been proposed: (1) the order-to-disorder (ODT) transition and (2) hydrodynamic clustering. The ODT theory was developed by Whitlock and Metzner [14] and then verified by Hoffman [9,11]. The theory holds that the repulsive particle–particle interactions keep the particles in an ordered, layered, and equilibrium structure when shearing a concentrated stabilized solution at a relatively low shear rate. However, when the shear rate elevates above the critical shear rate (i.e. when the ratio of the hydrodynamic forces to the repulsive forces, which can be Brownian or electrostatic, is higher than one), shear forces push the particles together to overcome the repulsive particle–particle interactions, forcing the particles out of their equilibrium positions. This leads to a disordered structure, causing an increase in viscosity.

Bossis and Brady developed the hydrodynamic clustering theory based on Stokesian's dynamic model [15]. Hydrodynamic clustering theory holds that when the particles of a stabilized suspension transfer from an immobile state to a mobile state, small groupings of particles form hydro-clusters, increasing the suspension's viscosity. These hydro-clusters are composed of particles that are momentarily compressed together, forming an irregular, rod-like chain of particles akin to a logjam or traffic jam. In theory, these particles have extremely small interparticle gaps, rendering these momentary and transient hydro-clusters as an incompressible structure. The commonly accepted picture of shear thickening in Brownian suspensions has been the formation of shear-induced hydro-clusters.

Stokesian dynamics is a molecular dynamics-like method for simulating the behavior of many particles suspended in a fluid. This method treats the suspended particles in a discrete sense, while the continuum approximation remains valid for the surrounding fluid, that is the suspended particles are generally assumed to be significantly larger than the molecules of the solvent. The particles then interact with hydrodynamic forces transmitted through the continuum fluid when the Reynolds number of the particles is small. These forces are determined by the linear Stokesian equations. In addition, the method can also resolve non-hydrodynamic forces, such as Brownian forces arising from the fluctuating motion of the fluid, and interparticle or external forces. Thus, Stokesian dynamics can be applied to a variety of problems, including sedimentation, diffusion, and rheology. It aims to provide the same level of understanding for multiphase particulate systems as molecular dynamics does for statistical properties of matter.

It has been widely accepted in the hydro-cluster theory that transient concentration fluctuations are driven and sustained by the applied shear field. The viscosity increase is continuous at low volume fractions. Shear thickening is also observed in non-Brownian suspensions with larger particle sizes [16–23]. Here, the mechanisms at play are still not clear.

In the concrete industry, it has been accepted that the shear thickening phenomena occur with the initiation of the finest particles due to shear-induced microstructural changes in the composite [24]. However, for fluid cementitious composites, such as SCC, aggregate particles are able to flow freely in the fluid matrix, and particle friction and collision are essential. As discussed previously, the hydro-cluster theory may be applicable at the macroscopic level too. Therefore, a fundamental understanding of the process of shear thickening of SCC at the macroscopic level is necessary and may provide a strategy to minimize this effect.

Recently, a rheological model for predicting the flow behavior of a fluid mortar

was developed [25]. In this model, the fluid mortar is considered as a two-phase suspension with fine aggregate particles dispersed in a cement paste. The shear stress of the mortar is assumed to be the sum of the shear stresses resulting from the paste flow, the aggregate particle collisions, and the interactions between the cement paste and aggregate. Because concrete can be considered as coarse aggregate particles dispersed in a mortar, this model is also applicable for SCC. It should be emphasized that when concrete is flowing, different constituent phases experience different shear rates. The global concrete shear rate varies from 10 to 100 s^{-1} when SCC is mixing, flowing, or pumping. The SCC components, such as cement paste, generally experience a higher shear rate than the global concrete shear rate [25,26].

Detailed information about the model's development has been presented in a previous paper [25]. In this article, the critical component of the proposed model, the number of aggregate particle collisions in a flowing mortar, is modified and discussed in detail. This modified model explains the rigid particle collisions occurring in the process of the shear thickening of the bulk material at the macroscopic level. To support this view and validate the model, experimental work was conducted on top of a previous study [6].

2. Review of model development

In this article, a previously developed particle–fluid model [25] is used to predict the relationship between the shear stress and shear strain rate of self-consolidating mortar. This section presents key components of the model development, while more details can be found in [25]. In the model, the following assumptions have been made for predicting the flow behavior of a highly flowable mortar:

1. All aggregate particles in the mortar are rigid, spherical particles with an average diameter D and average interparticle distance S, where $S = [(1-1.35V_A)/(3\ V_A)]\cdot D$ and (V_A) is the volume fraction of aggregate in the mortar.
2. The mortar is an ideal viscous material, and the shear generated between the mortar layers is in the horizontal direction.
3. When the mortar flows, collisions will occur among the aggregate particles. The moving aggregate particles have a mean flow velocity (V_M) and a fluctuation velocity (V_F).
4. There is no static and dynamic segregation in the mortar.

The overall shear stress of a flowing SCC mortar (τ_M) is assumed to be the sum of the shear stress resulting from (1) the yield stress of the paste ($\tau_{P\ 0}$), (2) the flow of the paste (τ_P), (3) the interaction between the paste and aggregate ($\tau_{A\text{-}P}$), and (4) the shear stress resulting from the aggregate collisions (τ_A). This can be expressed by Equation (1):

$$\tau_M = \tau_{p0} + \tau_p + \tau_{A-P} + \tau_A \qquad (1)$$

The yield stress of paste ($\tau_{P\ 0}$) can be determined from a rheological test or a prediction model [27]. The shear stress from the paste flow (τ_P) is provided by its viscosity (η_P), the global shear rate of the mortar ($\dot{\gamma}_M$), and the volume fraction of aggregate particles in the mortar (V_A):

$$\tau_P = \eta_P \cdot \dot{\gamma}_M \cdot \frac{1 + 1.65V_A}{1 - 1.35V_A} \cdot (1 - V_A) \qquad (2)$$

The shear stress resulting from the interaction between the paste and aggregate ($\tau_{A\text{-}P}$) is considered to be $\tau_{A\text{-}P} = (k_P \cdot F_{FP}) \cdot N_{collision}$, where F_{FP} is the normal force that a single moving aggregate particle applies to the paste in front of these particles; k_P is the normal stress coefficient; and $N_{collision}$, also called number of aggregate collision, is the number of particles that move from their host shear plane onto the adjacent plane so as to cause

particle collisions in the other shear plane. The normal force (F_{FP}) applied to the paste around a moving particle is equal to the drag force applied by the paste on the moving particles in terms of magnitude, but in the opposite direction, and is given by $F_{FP} = C_D \rho_P \frac{V_F^2}{2} A$. In this equation, C_D is the coefficient for the mortar dragging force, ρ_P is the paste density, V_F is particle fluctuation velocity, and A is the projected area of a spherical aggregate particle ($A = \pi D^2/4$, where D is the average diameter of the particles).

The shear stress resulting from the aggregate movement (τ_A) can be described as $\tau_A = N_{collision} \cdot (\Delta P_X)$, where $N_{collision}$ is the number of colliding particles, and (ΔP_X) is the momentum change per one collision by two particles. While the continuum approximation remains valid for the surrounding fluid, the energy dissipation (ζ) during a solid particle collision is proportional to the shear stress generated by the collision (τ_A), which, in turn, is proportional to the momentum change of the colliding particles (ΔP_X).

Based on the first law of thermodynamics, the energy dissipation (ζ) is also a sum of the energy loss directly due to the particle collision ($\Delta E_{collision}$) and the energy loss due to the interaction between the aggregate particle and the mortar ($\Delta E_{interaction}$):

$$\zeta = \tau_A \frac{\partial u}{\partial y} = \left(N_{collision} \cdot \Delta P_X \frac{\partial u}{\partial y} \right) \quad (3)$$

$$\zeta = \Delta E_{collision} + \Delta E_{interaction} \quad (4)$$

where ∂_u/∂_y is the velocity gradient.

By solving Equations (3) and (4), the fluctuation velocity V_F can be obtained. As a result, the shear stress generated in a mortar (Equation (1)) can be rewritten as Equation (5):

$$\tau_M = \tau_{P0} + \eta_P \cdot \dot{\gamma}_M \cdot \frac{1 + 1.65V_A}{1 - 1.35V_A} \cdot (1 - V_A) + 1.9098 \cdot \frac{k_P \cdot C_D \cdot \rho_P \cdot V_F^3 \cdot V_A^2 \cdot A}{D^3 \cdot (1 + 1.65V_A)} + 3.8196 \cdot \frac{V_A^2 \cdot V_F}{D^3} \cdot \frac{1}{1 + 1.65V_A} \cdot (\Delta P_X) \quad (5)$$

The viscosity of mortar can be obtained, based on its rheological definition, as $\eta_M = \tau_M / \dot{\gamma}_M$.

3. Assessment of number of collisions in a fluid mortar

The key issue in use of the aforementioned model is to assess the number of collisions that may occur between unit adjacent horizontal planes in unit time, $N_{collision}$. According to Fabrice et al. [24], the number of collisions in unit time is determined by the function of the average aggregate diameter, (D), volume fraction (V_A), and particle fluctuation velocity (V_F) as follows:

$$N_{collision} = 3.8196 \cdot \frac{V_A^2 \cdot V_F}{D^3} \cdot \frac{1}{1 + 1.65V_A} \quad (6)$$

Based on Equation (6), for a given average particle diameter and fluctuation velocity, the number of collisions $N_{collision}$ increases with the aggregate volume fraction (V_A) (Figure 1).

For a constant aggregate volume fraction (V_A) and fluctuation velocity (V_F), the number of collisions $N_{collision}$ decreases with increased average particle diameters (Figure 2) because of the increased interparticle distance. For a given volume fraction (V_A) and average diameter (D), the number of collisions $N_{collision}$ also increases with the particle fluctuation velocity (V_F) (Figure 3).

The trends presented in Figures 1 through 3 are in good agreement with the general concept of particle movement. They indicate that the equation for assessing the number of collisions in a fluid mortar (Equation (6)) is rational.

4. Study of factors that affect shear thickening using the modified model

In the present study, the above-mentioned model was used to study the factors that affect shear thickening potential in flowing cementitious composites. To simplify the model, Equation (5) can be rewritten as the

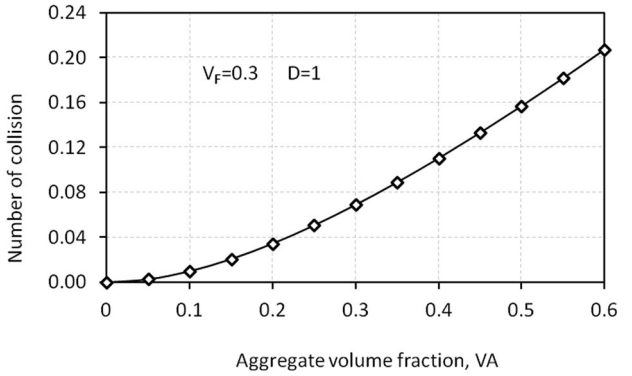

Figure 1. The effect of aggregate volume fractions on number of collisions.

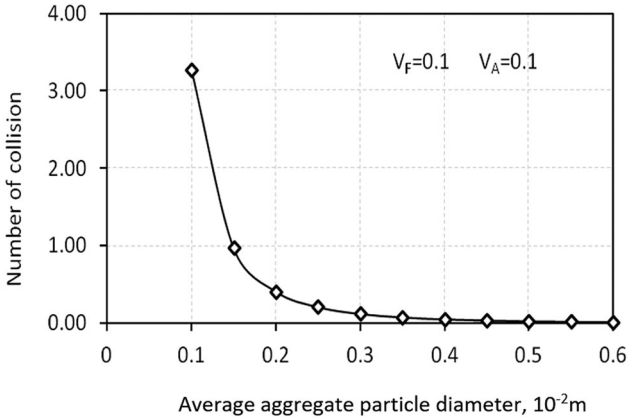

Figure 2. The effect of average aggregate particle diameters on number of collisions.

following:

$$\tau_M = \tau_0 + A \cdot \dot{\gamma} + B \cdot \dot{\gamma}^2 + C \cdot \dot{\gamma}^3 \qquad (7)$$

where A, B, and C are constant factors related to the mortar's material properties and can be calculated from the equations provided in Section 3 of this article. The yield value τ_0 is a real yield value, and $\dot{\gamma}$ is the global shear rate of mortar. Equation (7) shows that the new particle–fluid model has a power format similar to both the modified Bingham model proposed by Feys et al. and experimental data from SCC rheology tests [5].

In mathematics, solutions to Equations (3) and (4) include two roots, positive and negative values. Depending on the different constitute materials used, such as cement paste, only one solution to the equations is applicable. The physical meaning of a negative root means that the particle flowing in a fluid medium is limited to a low level. Continued shearing of the mortar will not dissipate additional external energy, and the overall energy in a flowing suspension decreases, which leads to shear thinning behavior. Given a highly flowable fluid medium, particles are able to flow easily in it, and the collisions between adjacent layers are dominant. In this case, positive particle velocity is present. Due to the collisions of particles with high speeds, the magnitude of energy and the possibility of particle collision increase the shear stress at which shear thickening starts. The model presented in this article extends the

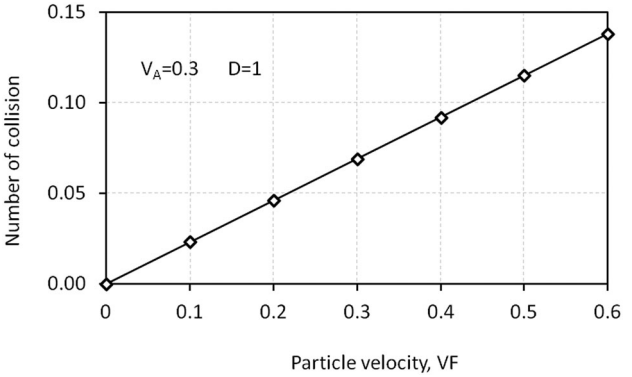

Figure 3. The effect of aggregate particle velocities on number of collisions.

modified Bingham model proposed by Feys et al. with a cubic term [5]. From the authors' study, the quadratic and cubic terms in the monic cubic polynomial (Equation (7)), as well as the second order term in Feys et al.'s modified Bingham model, are due to particles flowing in a fluid medium, such as interparticle collisions and interactions between particles and cement paste.

Two types of inputs are utilized in the particle–fluid model. One is the material property inputs, which can be determined from the actual mix proportion of the mortar tested, such as the average diameter (D) and volume fraction (V_A) of aggregate and the density (ρ_P), yield stress (τ_{P0}), and viscosity (η_P) of paste. The second is a group of dimensionless parameters, such as friction coefficient of the aggregate (μ), coefficient of elastic restitution (ε), and coefficient of drag of cement paste (C_D). Due to difficulties in determining the dimensionless parameters, only a parametrical study was completed to examine the effects of material properties on shear thickening of fresh mortar. The model was utilized to study the flow behavior of a fluid mortar in which the cement paste has an extraordinarily high flowability. For this reason, small magnitudes were adopted for the values of the parameters related to particle friction, such as k_P and μ.

4.1. *The effect of aggregate content*

To investigate the effect of aggregate content on shear thickening of SCC mortar, one cement paste ($\tau_0 = 0$Pa, $\eta = 0.10$ Pa.s), one aggregate size (D = 0.0015m), and four volume fractions of aggregate (20%, 40%, 50%, and 60%) are considered. The water-to-cement ratio (w/c) is fixed at 0.30. As shown in Figure 4, the flow curves of SCC mortars with different aggregate contents are significantly different. When the aggregate content increases, both the shear stress and viscosity of the mortar increase. This is caused by the higher degree of friction and collision of solid particles, based on which the intensity of shear thickening increases with the increasing volume fraction of suspended Brownian particles, as observed by Maranzano and Wagner [28].

The effects of aggregate contents on the mortar shear stresses and viscosities at a constant shear rate of $100\,s^{-1}$ are summarized in Figure 5. It is observed in the figure that at a low aggregate volume fraction (20% and 40%), the differences in the mortar's rheological parameters (shear stress and viscosity) resulting from different aggregate contents are not significant. However, the shear stress increases significantly when the aggregate content is higher than 50%.

In summary, the present particle–fluid model predicting rheological behavior has shown a possible source of shear

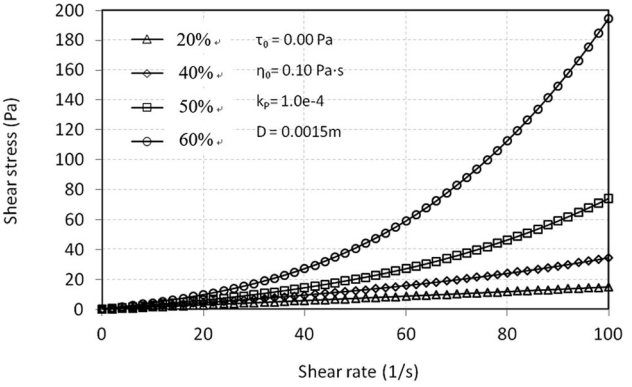

Figure 4. The effect of fine aggregate volume fractions on mortar shear stress.

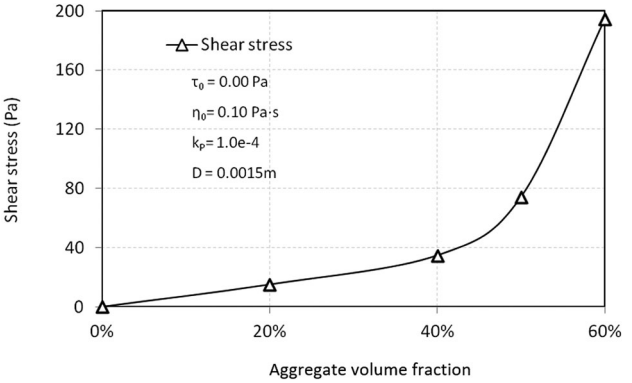

Figure 5. Relationship between fine aggregate volume fractions and SCC mortar shear stress at a constant shear rate of $100\,s^{-1}$.

thickening due to particle interactions at the macroscopic level. However, in order to initiate the shear thickening behavior, the matrix fluid should have a very high flowability to ensure the free and easy movement of aggregate particles in the fluid. The investigation of rigid spheres in contact leads to the idea that, at the macroscopic level, shear thickening can also be understood as a stress-induced transition in a jammed state. Based on the theoretical approach presented in this article, continuous shear thickening can be obtained at the macroscopic level. Shear thickening is significant at high volume concentrations of aggregate particles. For a mortar with a low aggregate volume fraction, the effect of aggregate volume fraction on the SCC mortar's shear thickening is not significant, but this effect becomes significant as the volume fraction of aggregate increases. All findings are consistent with the experimental results from mortar rheology tests [5,6].

4.2. The effect of cement paste aging on shear thickening

The basic cement properties used in the present model are yield stress and viscosity. These two basic rheological parameters are predominated by cement properties, the water-to-cement ratio (w/c), and the paste mixing method. To study the effect of cement paste aging on the rheological behavior of a SCC mortar, the same SCC mortar samples with different cement paste properties at two different times ($t_1 = 0\,s$ and $t_2 = 600\,s$) were studied. The volume

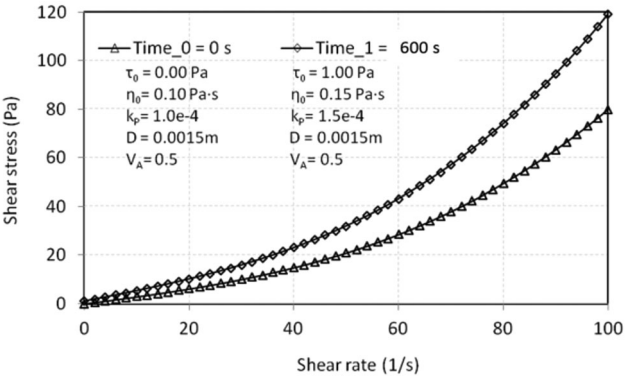

Figure 6. The effect of aging time on mortar shear stress.

fractions of aggregate particles in the mortar samples were set as 50%, and the average diameter of the aggregate particles was 0.0015 m. To simulate the different rheological properties of the same paste samples at different times, the physical properties, such as yield stress, viscosity, and friction coefficient, were adjusted to represent the different rheological behaviors for the same paste at different times. The representative shear stress and shear rate relationship with corresponding parameters is shown in Figure 6.

Figure 6 shows the flow curves derived from the present model for the mortars made with different aging times of cement paste. As observed in Figure 6, both the yield stress and viscosity of the mortars increase as time elapses. At a high shear rate, the increase in shear stress is more significant than at a low shear rate. This indicates that a larger force is required to initiate the mortar flow and to maintain a high flow rate, which is consistent with published results of mortar rheology testing and modeling [5,6].

5. Research significance

Shear thickening is a behavior of a material that displays an increase in viscosity with increasing shear rate. Although it can be gradual, this phenomenon may lead to a discontinuous jump in viscosity. A production engineer may be confronted with extreme shear thickening during increasing productivity by increasing line speed in a coating operation. When shear thickening occurs, it becomes more difficult to mix and pump concrete because of the increased energy required for concrete flow. In many cases, this undesirable shear thickening behavior limits the application of SCC where pumping is essential. It is of great significance to establish a model that explains the rigid particle collisions occurring in the process of the shear thickening of the bulk material at the macroscopic level.

6. Experimental work

Shear thickening behavior has been observed clearly in SCC mortar and noticeably in concrete mixtures [5,6]. To verify the theoretical work discussed in Section 4, the SCC mixtures used by Feys et al. were reproduced. In addition, rheology tests were performed on both the mortars and cement pastes of these SCC mixtures; these tests were not included in the previous study [5]. The details of the experimental work are presented next.

6.1. Materials, proportions, and mixing procedures

Paste and mortar samples were prepared with ordinary Portland cement (OPC), class

Table 1. Chemical properties of cementitious materials.

Major oxide composition, %	CaO	SiO_2	Al_2O_3	Fe_2O_3	MgO	SO_3	LOI
Portland cement	62.00	20.30	4.27	3.02	3.10	2.86	2.22
Class C fly ash	25.15	36.71	19.42	6.03	4.77	1.97	0.18

Table 2. Mixture proportions of mortar used in this study.

Mixture	PC (kg/m^3)	FA (kg/m^3)	AEA (ml/m^3)	HRWR (ml/m^3)	Fine Agg. (kg/m^3)	w/cm	V_A
SCC mortar 1 [6]	498	175	120	5811	1216	0.30	0.42
SCC mortar 2	498	175	120	5811	690	0.30	0.30
SCC mortar 3	498	172	120	5811	415	0.30	0.20

C fly ash, and different chemical admixtures. The main chemical compositions of the Portland cement and class C fly ash are shown in Table 1. The chemical admixtures were air-entraining agent (AEA) and polycarboxylate-based high range water reducer (HRWR). Material constituents and mixture proportions are tabulated in Table 2. The fine aggregate with a gradation satisfying ASTM C33 size number 8 was natural river sand with specific gravity of 2.68, fineness modulus of 2.80, and a water absorption value of 0.9% [29]. The morphology-based indices analysis was referred to Li et al. [30]. Other than the SCC mixture proportion used in [6] (SCC mortar 1 in Table 2), two more mortar mixture proportions with different volumetric fractions of aggregate particles were adopted, that is SCC mortar 2 with V_A=0.3 and SCC mortar 3 with V_A=0.2. All cement paste and mortar samples were prepared in accordance with ASTM C305. The temperatures for mixing water and cement were controlled at 25 °C (77 °F). The environmental temperature and relative humidity during the paste mixing and testing were 25 ± 1.5 °C (77 ± 2.7 °F) and 50 ± 3%, respectively.

6.2. *Test methods*

A Brookfield R/S SST200 rheometer was used to measure the rheology parameters of the cement pastes as shown in Figure 7 (top). The sample was placed in a 50 mm diameter × 100 mm tall cylindrical vessel and sheared with a 15 × 30 mm vane spindle. The capacity of the torque for the rheometer ranges from 1.5 to 50 mN·m. The loading history adopted in the experimental studies is shown in Figure 7 (bottom). The loading initially ramped up the spindle rotation from 0 to 0.2 s^{-1} over 180 s, and the rotation was then sustained at 0.2 s^{-1} for 60 s. The spindle rotation was subsequently increased from 0.2 to 100 s^{-1} over 60 s and reduced to 0 s^{-1} over the following 60 s. Tests were conducted every 15 min from 15 to 90 min to capture both shear stress and viscosity. It should be noted that the use of a vane geometry in the wide-gap rheometer configuration in order to study the viscoelastic behavior of cement paste or mortar suspensions requires the computation of both the shear stress and shear rate from the torque and rotational speed, respectively. The long-standing problem in rheometry is the so-called "Couette inverse problem" and for the Bingham fluid the conversion equation is known as the "Reiner–Rivlin" equation. However, the derivation of both the shear stress and shear rate from direct measurements of torque and rotational speed is beyond the scope of this study. The integration method, that is the type of constitutive equation, is specified in the software associated with Brookfield R/S SST200

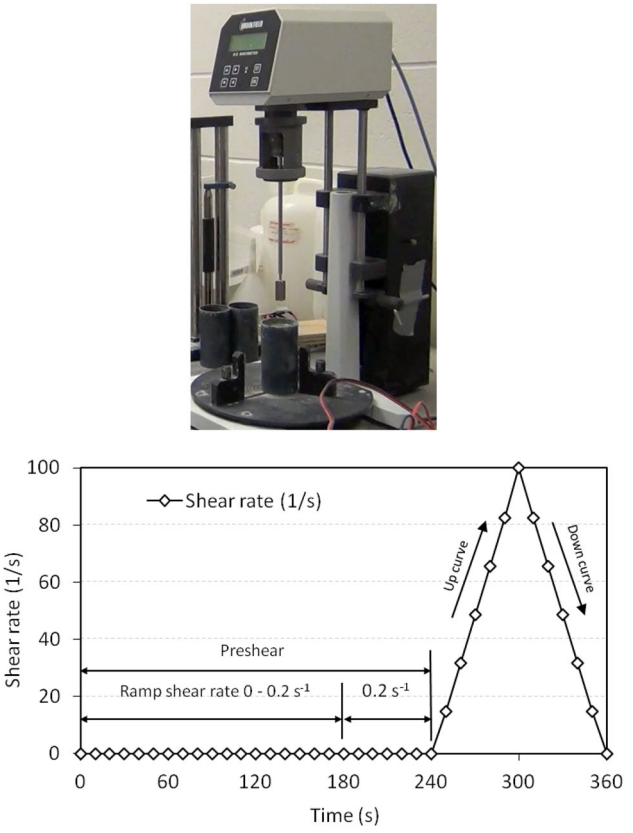

Figure 7. The Brookfield R/S SST200 rheometer (top) and loading history with pre-shear (bottom).

rheometer and integrated to obtain shear stress and shear rate relationship, which is fitted to the experimental data as described in [31]. Therefore, the output data from the rheometer used in this study are defaulted as shear stress versus shear rate.

6.3. *Results and discussion*

The flow curves for the SCC mortar mixtures from the down-curve at different elapsed times after mixing are provided in Figure 8(a) [6]. The shear thickening behavior of the SCC mortar is clearly observed in the down-curve of the flow curve. The flow curves for the SCC paste mixtures are provided in Figure 8(b). However, no significant shear thickening behavior of the SCC paste can be observed in the down-curve of the flow curve. Considering that the shear rate applied to the cement paste is about two to three times higher than the global shear rate of the mortar in the case of SCC [26], the shear curves for SCC paste between the shear rates of 0 to 100 s^{-1} are representative of the shear curves of SCC mortar between the shear rates of 0 to 40 s^{-1}. Because no significant shear thickening is observed in SCC paste up to a shear rate of 100 s^{-1} while shear thickening seems to occur in SCC mortar at shear rates between 0 and 40 s^{-1}, it is therefore reasonable to assume that the shear thickening observed in SCC mortar is mainly due to interactions among the aggregate particles, for example collision and friction.

The yield stresses and viscosities of SCC pastes at different times after mixing

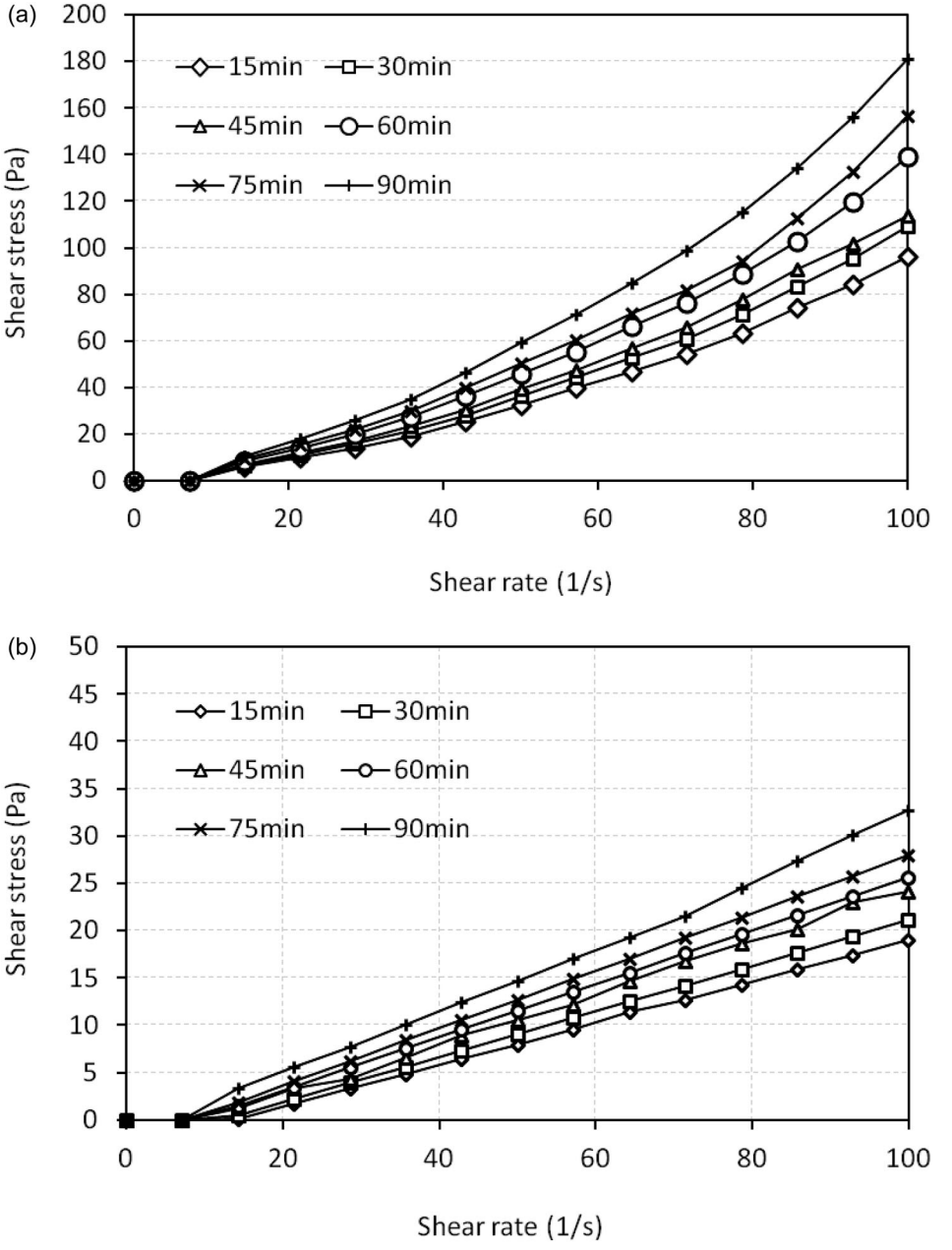

Figure 8. (a) The effect of elapsed times on flow curves (down-curve) of SCC mortar [6]. (b) The effect of elapsed times on flow curves (down-curve) of SCC paste.

were obtained from the flow curves in Figure 8(b) and are tabulated in Table 3. These values were applied to obtain flow curves using Equation (5). Aggregate volume fraction (V_A) and average particle diameter (D) were determined through mixture design and sand size distribution. Dimensionless parameters, other than k_P, were the same as those used in Section 4. The dimensionless parameter, k_P, was obtained by linear interpolation between the value of 0.0001 at 15 min after mixing

Table 3. Rheological properties of SCC pastes at different times after mixing.

Time (min)	15	30	45	60	75	90
Yield stress (Pa)	0.00010	0.00011	0.00012	0.00012	0.00013	0.00014
Viscosity (Pa·s)	0.179	0.200	0.232	0.247	0.270	0.313

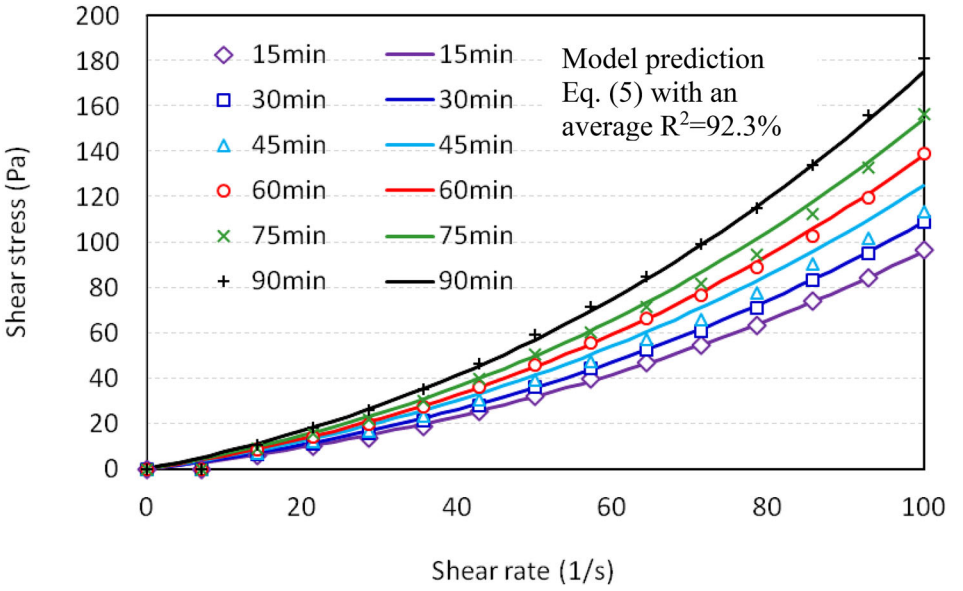

Figure 9. The comparison of flow curves with different elapsed times from experimental results (symbols) [6] and model predictions (lines).

and 0.00014 at 90 min after mixing. The flow curves of both the model's predictions (Equation (5)) and the results of experimental work (Figure 8(a)) are provided in Figure 9, in which the symbols represent the test results and the lines represent the model-predicted continuous flow curves. The overlap indicates that the agreement is satisfactory for the shear rate applied in this study. The model predicts a nonlinear increase in the shear stress with the shear rate for various elapsed times after mixing, especially at high volumetric fractions of aggregate particles, which fits the experimental data well with an average R^2 of 92.3%.

Four mixtures of mortar with the same paste but different volumetric fractions (0%, 20%, 30%, and 40%) were designed to further test the effects of solid volumetric fractions. Due to experimental limitations, no test was completed successfully at aggregate volumetric fractions higher than 40%. The flow curves for the SCC mortar mixtures from the down-curve at different times after mixing are presented in Figure 10. Again, the model-predicted (Equation (5)) relationship between shear stress and shear rate, presented as continuous flow curves, is in agreement with the test results, presented as symbols. The regression coefficient R^2 values for each volume fraction are given in the figure as well. The shear thickening behavior of the SCC mortar is clearly shown in the down-curve of the flow curve when the aggregate volumetric fraction is greater than 30%. The evolution of the viscosity as a function of the shear rate is reported in Figure 11. No shear thickening is clearly seen in the paste sample (V_A=0); even shear thinning behavior can be observed. However, when

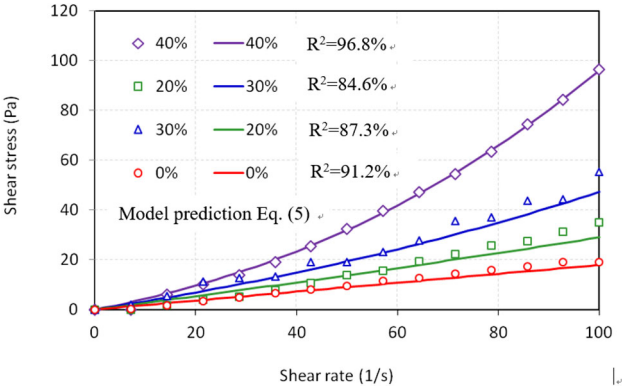

Figure 10. The flow curves of aggregate volume fractions over the shear rate: experimental results (symbols) and model predictions (lines).

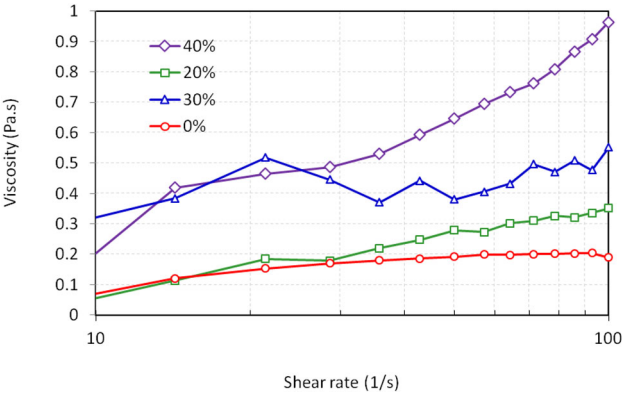

Figure 11. The effect of aggregate volume fractions on viscosity of mortar at various shear rates.

the aggregate volumetric fraction increases, shear thickening occurs. Clear inflection points were observed for mortar mixtures (V_A=20%, 30%, and 40%) between the shear rates of 40 and 60 s^{-1}. It should be noted that the extraordinary viscosity of the 30% aggregate volume fraction at the shear rate of around 22 s^{-1} might be an outlier from the rheology testing process.

7. Conclusions

In this rheology study on SCC, shear thickening behaviors were observed in mortar rheology tests for SCC, although no shear thickening was observed in the paste rheology tests. The following conclusions can be drawn from this study:

- Based on the rheology test results, no apparent shear thickening behavior was observed for SCC paste mixtures. However, when fine aggregate was introduced to produce SCC mortar, the relationship between shear stress and shear rate started to exhibit shear thickening behavior. This behavior became distinct when the fine aggregate volume fraction was increased up to 40%. The inflection point of shear thickening behavior generally occurred between the shear rates of 40 and 60 s^{-1}.
- The particle–fluid model, developed for studying the flow behavior

of highly flowable mortar, was modified and utilized to better understand the phenomenon and quantitatively predict the rheological behavior of SCC mortar. The modified model showed a power function between the shear stress and shear rate that could well capture the shear thickening behavior of mortar mixtures with various aggregate volume fractions and that agreed well with the results of the rheology study.

- Based on the present modeling study, at the macroscopic level, shear thickening behavior occurred because of the particle interactions in the cement-based system, such as collision and friction, and aggregate–paste interaction during shearing. Given the high flowability of the paste fluid, aggregate particles were able to flow freely in the paste fluid. With the collision and friction occurred at high speeds, aggregate particles could generate local transient particle clusters due to the particles' varying velocities. Hence, shear thickening occurred.
- Only shear thickening behaviors were observed at the macroscopic level for the SCC mortar tested in this study. The critical shear rate, after shear thickening occurred, was not observed in the present experiment, which was in good agreement with the model predictions.

List of symbols

A	projected area of a sphere aggregate particle
C_D	coefficient of the cement paste dragging force
D	average diameter of aggregate particles
(ΔP_X)	momentum change per one collision by two particles
$\Delta E_{collision}$	total energy loss due to particle collision
$\Delta E_{interaction}$	energy loss due to interaction between the aggregate particle and cement paste
F_{FP}	force acting on cement paste by a single aggregate particle
k_P	normal stress coefficient
m	average mass of aggregate particles
$N_{collision}$	number of aggregate collision
S	average distance between the aggregate particles in mortar
V_A	volume fraction of aggregate
V_F	magnitude of particle fluctuation velocity
ε	coefficient of elastic restitution
ρ_P	cement paste density
ζ	energy dissipation, which is always positive definite
η_P	viscosity of the cement paste in mortar
η_M	mortar viscosity
$\dot{\gamma}_M$	apparent shear rate of the mortar
$\dot{\gamma}_P$	apparent shear rate of cement paste
τ_M	shear stress of mortar
τ_{P0}	yield stress of the cement paste
τ_P	shear stress resulting from the cement paste flow in mortar
$\tau_{A\text{-}P}$	shear stress due to the aggregate–cement paste interaction
τ_A	shear stress generated by the fine aggregate movement
μ	friction coefficient of particles
∂_u/∂_y	velocity gradient of mortar

Acknowledgements

The authors would like to express his sincere thanks to Professor Nemkumar Banthia at the University of British Columbia for his valuable input and discussions on this article.

Disclosure statement

The authors declare that they have no conflict of interest.

Availability of data and material

The authors agree to share their data.

Funding

This work was partially supported by Portland Cement Laboratory in Civil Engineering Department at Iowa State University, Ames, Iowa, United States. This study was also partially supported by the National Natural Science Foundation Project (NSFC 51868066, 51908057). The Science and Technology Projects of Gansu Transportation Department (Grant No. 2019-16 and Grant No. 2019-17), Opening Foundation of Research and Development Center of Transport Industry of Technologies, Materials and Equipments of Highway Construction and Maintenance (Gansu Road & Bridge Construction Group), China (Grant No. GLKF201807).

References

[1] Okamura H, Ouchi M. Self-compacting concrete. ACT. 2003;1:5–15.
[2] Ouchi M, Hibino M, Okamura H. Effect of superplasticizer on self-compactability of fresh concrete. Transportation Res Rec. 1997;1574:37–40.
[3] Edamatsu Y, Nishida N, Ouchi M, et al. A rational mix-design method for self-compacting concrete considering interaction between coarse aggregate and mortar particles. Int RILEM Symp Self-Compacting Concr, Stockholm, SUEDE. 1999;309–320.
[4] Quadrat O. Negative thixotropy in polymer solutions. Adv Colloid Interface Sci. 1985;24:45–75.
[5] Feys D, Verhoeven R, DeSchutter G. 2006. Fundamental study of the rheology of self-compacting concrete, composed with Belgian materials. In: The 7th National Congress on Theory and Applied Mechanics (NCTAM).
[6] Lomboy GR, Wang X, Wang K. Rheological behavior and formwork pressure of SCC, SFSCC, and NC mixtures. Cem Concr Compos. 2014;54:110–116.
[7] Boersma WH, Laven J, Stein HN. Shear thickening (dilatancy) in concentrated dispersions. AIChE J. 1990;36:321–332.
[8] Franks GV, Zhou Z, Duin NJ, et al. Effect of interparticle forces on shear thickening of oxide suspensions. J Rheol. 2000;36:845–883.
[9] Hoffman RL. Discontinuous and dilatant viscosity behavior in concentrated suspensions. I. observation of a flow instability. J Rheol. 1972;16:155–173.
[10] Macias ER, Bautista F, Soltero JFA, et al. On the shear thickening flow of dilute CTAT worm-like micellar solutions. J Rheol. 2003;47:643–658.
[11] Hoffman RL. Discontinuous and dilatant viscosity behavior in concentrated suspensions. II. Theory and experimental tests. J Colloid Interface Sci. 1974;46:491–506.
[12] Foss DR, Brady JF. Structure, diffusion and rheology of Brownian suspensions by Stokesian dynamics simulation. J Fluid Mech. 2000;407:167–200.
[13] Chen LB, Ackerson BJ, Zukoski CF. Rheological consequences of microstructural transitions in colloidal crystals. J Rheol. 1994;38:193–216.
[14] Metzner AB, Whitlock M. Flow behavior of concentrated (dilatant) suspensions. Trans Soc Rheol. 1958;11:239–254.
[15] Brady J, Bossis G. Stokesian dynamics. Annu Rev Fluid Mech. 1988;20:111–157.
[16] Williamson RV, Hecker WW. Some properties of dispersions of quicksand type. Ind Eng Chem. 1931;23:667–670.
[17] Fall A, Huang N, Bertrand F, et al. Shear thickening of cornstarch suspension as a re-entrant jamming transition. Phys Rev Lett. 2008;100:018301.
[18] Fall A, Lemaitre A, Bertrand F, et al. Shear thickening and migration in granular suspensions. Phys Rev Lett. 2010;105:268303
[19] van der Werff JC, De Kruif CG. Hard-sphere colloidal dispersion: the scaling of rheological properties with particle size, volume fraction, and shear rate. J Rheol. 1989;33:421–454.
[20] Sellitto M, Kurchan J. Shear-thickening and entropy-driven reentrance. Phys Rev Lett. 2005;95:236001.
[21] Berthier L, Barrat JL, Kurchan J. A two-time-scale, two-temperature

scenario for nonlinear rheology. J Phys Rev E. 2000;61:5464–5472.
[22] Brown E, Jaeger HM. Dynamic jamming point for shear thickening suspensions. Phys Rev Lett. 2009;103:086001.
[23] Brown E, Jaeger HM. The role of dilation and confining stresses in shear thickening of dense suspensions. J Rheol. 2012;56:875–923.
[24] Fabrice T, Cédric R, Pierre-Henri J. Reducing shear thickening of cement-based suspensions. Rheologica Acta. 2009;48:883–895.
[25] Lu G, Wang K, Rudolphi T. Modeling rheological behavior of a highly flowable mortar using concepts of particle and fluid mechanics. Cem Concr Compos. 2008;30:1–12.
[26] Roussel N. A thixotropy model for fresh fluid concretes: theory, validation and applications. Cem Concr Res. 2006;36:1797–1806.
[27] Lu G, Wang K. Experimental study on shear behavior of fresh mortar. Cem Concr Compos. 2011;33:319–327.
[28] Maranzano BJ, Wagner NJ. The effect of particle size on reversible shear thickening of concentrated colloidal dispersions. J Chem Phys. 2001;114:10514–10527.
[29] Wang X, Sadati S, Taylor P, et al. Material characterization to assess effectiveness of surface treatment to prevent joint deterioration from oxychloride formation mechanism. Cem Concr Comp. 2019;104:103394.
[30] Li C, Zheng J, Zhang Z, et al. Morphology-based indices and recommended sampling sizes for using image-based methods to quantify degradations of compacted aggregate materials. Constr Build Mater. 2020;230:116970.
[31] Heirman G, Vandewalle L, Van Gemert D, et al. 2006. Contribution to the solution of the Couette inverse problem for Herschel-Bulkley fluids by means of the integration method. In: 2nd International Symposium on Advances in Concrete through Science and Engineering, Quebec.